SNRs as PeVatron candidates for CTA

Ziwei Ou & Tiina Suomijarvi

Institut de Physique Nucléaire d'Orsay

Université Paris-Sud

2019|06|24

Content

- Reconstruction of DC-1 GPS data
- MWL fitting results using Naima package
- Summary

17 selected low Galactic latitude SNRsfrom TeVCat

SNR name	Galactic Longitude	Galactic Latitude	Type
HESS J1534−571	323.65	-0.92	Shell
HESS J1614+516	331.52	-0.58	Shell
RX J1713.7−3946	347.34	-0.47	Shell
CTB 37B	348.65	0.38	Shell
HESS J1731−347	347.34	-0.47	Shell
HESS J1912+101	44.39	-0.07	Shell
0FGL J1954.4+2838	65.30	0.38	Shell
SNR G318.2+00.1	318.36	-0.43	SNR/Molec. Cloud
CTB 37A	348.39	0.11	SNR/Molec. Cloud
SNR G349.7+00.2	349.72	0.17	SNR/Molec. Cloud
HESS J1745−303	358.71	-0.64	SNR/Molec. Cloud
HESS J1800−240C	5.71	-0.06	SNR/Molec. Cloud
HESS J1800−240B	5.90	-0.37	SNR/Molec. Cloud
W 28	6.66	-0.27	SNR/Molec. Cloud
HESS J1800−240A	6.14	-0.63	SNR/Molec. Cloud
W 49B	43.32	-0.16	SNR/Molec. Cloud
SNR G015.4+00.1	15.41	0.16	Composite SNR

Selected TeVCat sources in DC-1 Galactic Plane Survey simulation

SNR name	source type	spectrum type	spatial model type
RX J1713.7−3946	Diffuse Source	Exp. Cut-off Power Law	Diffuse Map
HESS J1614+516	Extended Source	Power Law	Radial Gaussian
HESS J1731−347	Extended Source	Power Law	Radial Shell
HESS J1912+101	Extended Source	Power Law	Radial Gaussian
HESS J1745−303	Extended Source	Power Law	Radial Gaussian
W 28	Extended Source	Power Law	Radial Gaussian
HESS J1800−240A	Diffuse Source	Power Law	Diffuse Map
W 49B	Point Source	Power Law	Power Source
W 51C	Extended Source	Power Law	Radial Gaussian

Ctools procedure

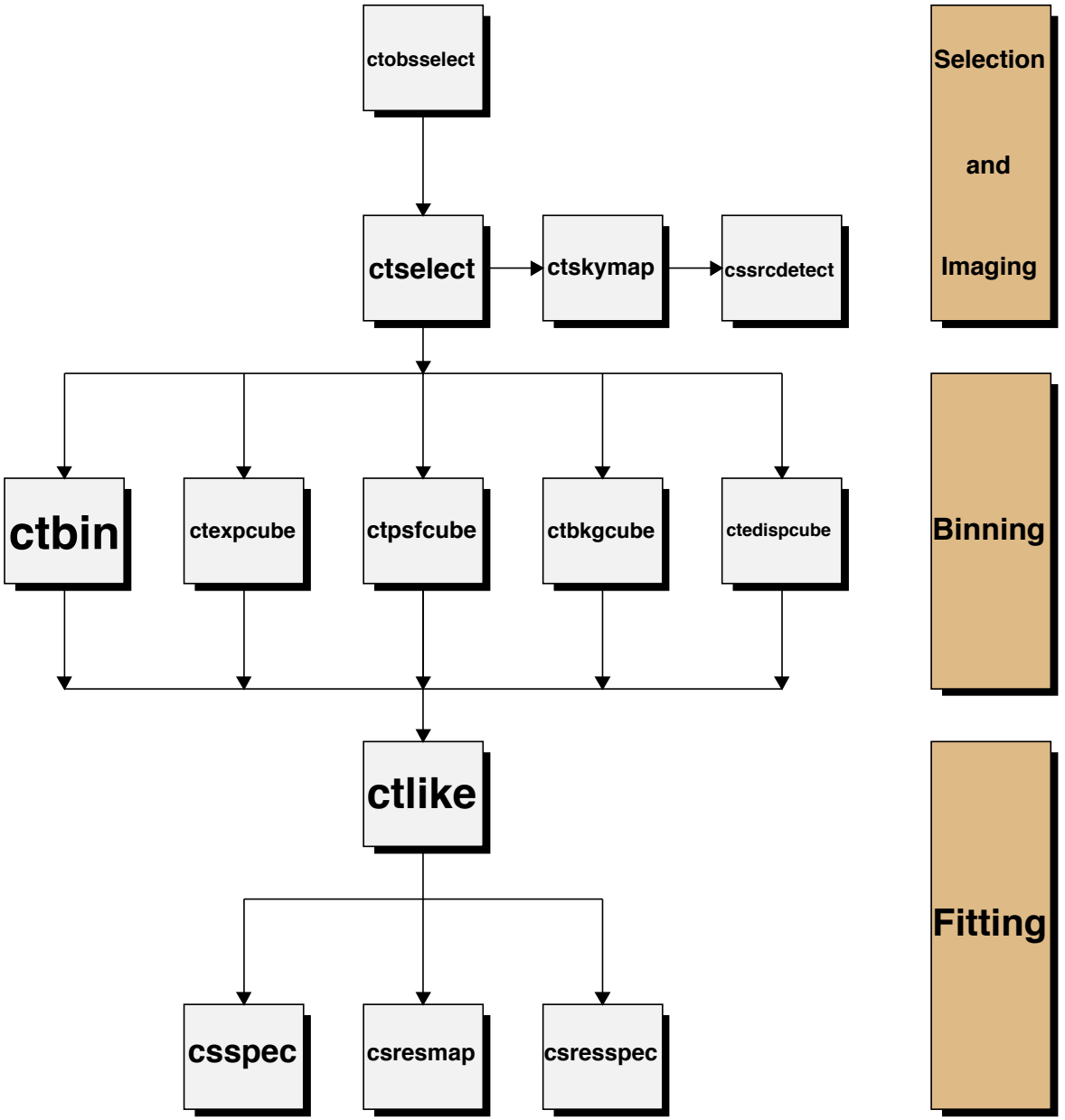

HESS J1614+516

Sky map

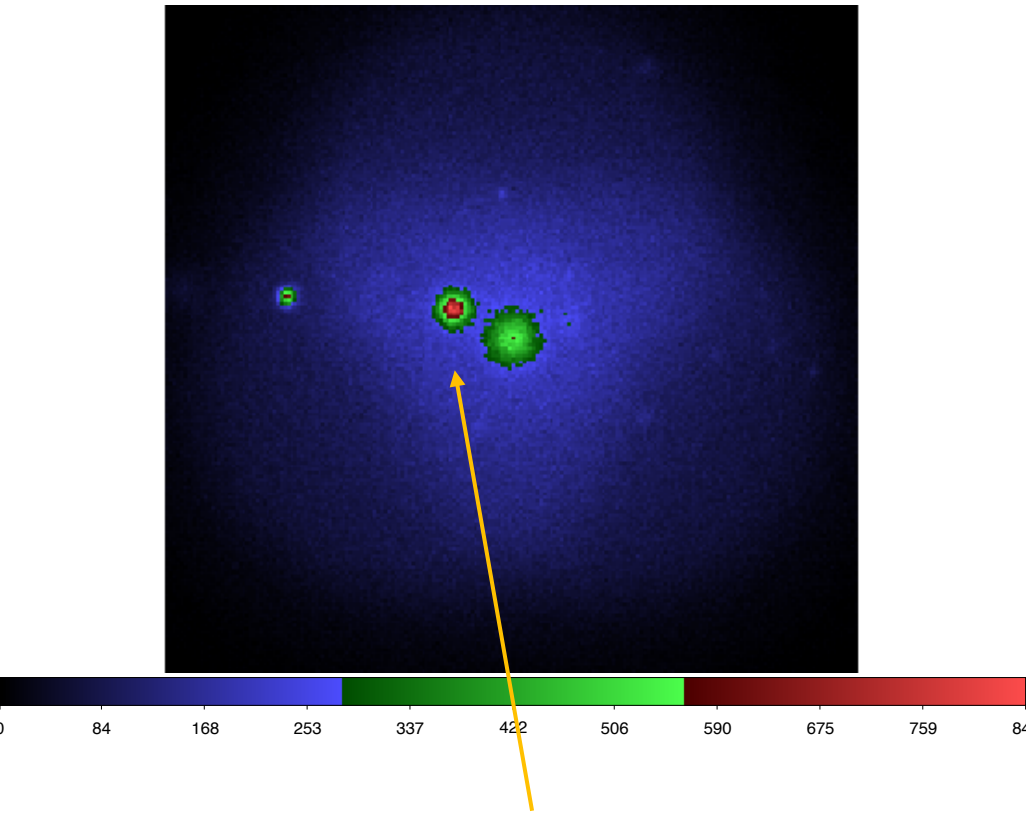

Residual map

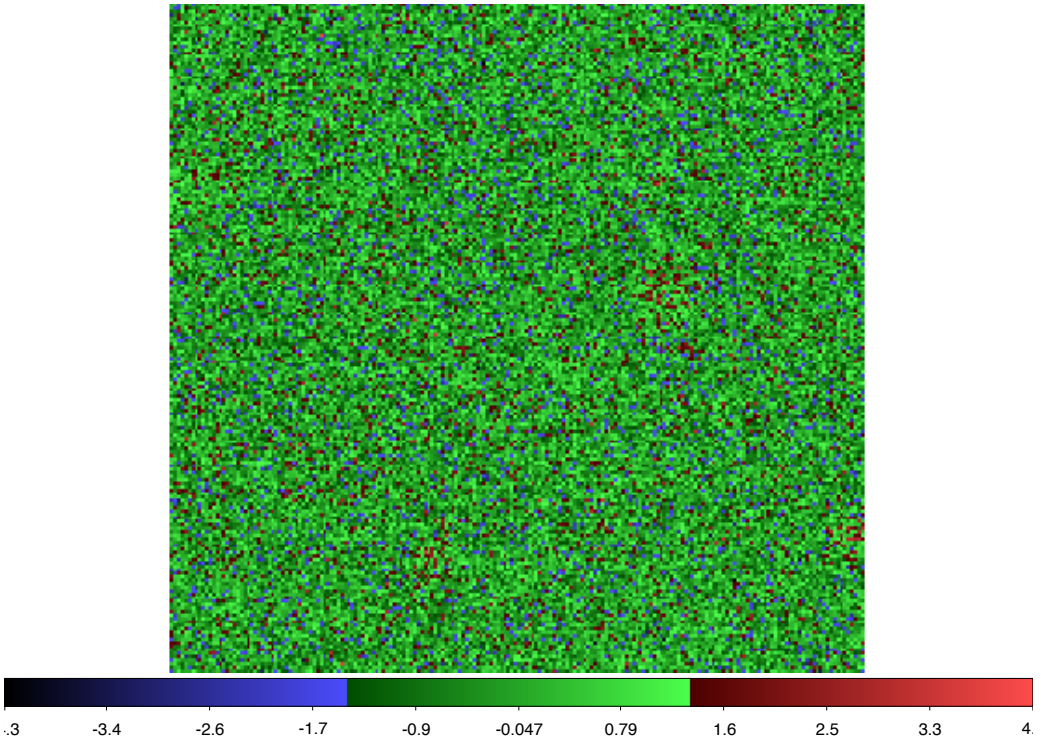

HESS J1616-508 also in the FoV

HESS J1614+516

Residual spectrum

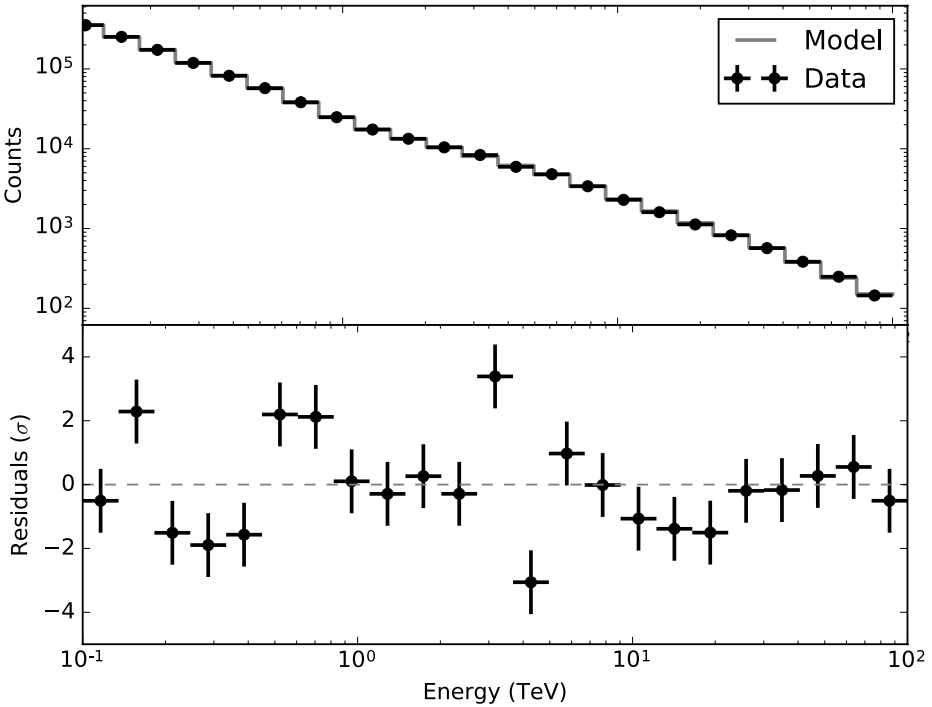

SED

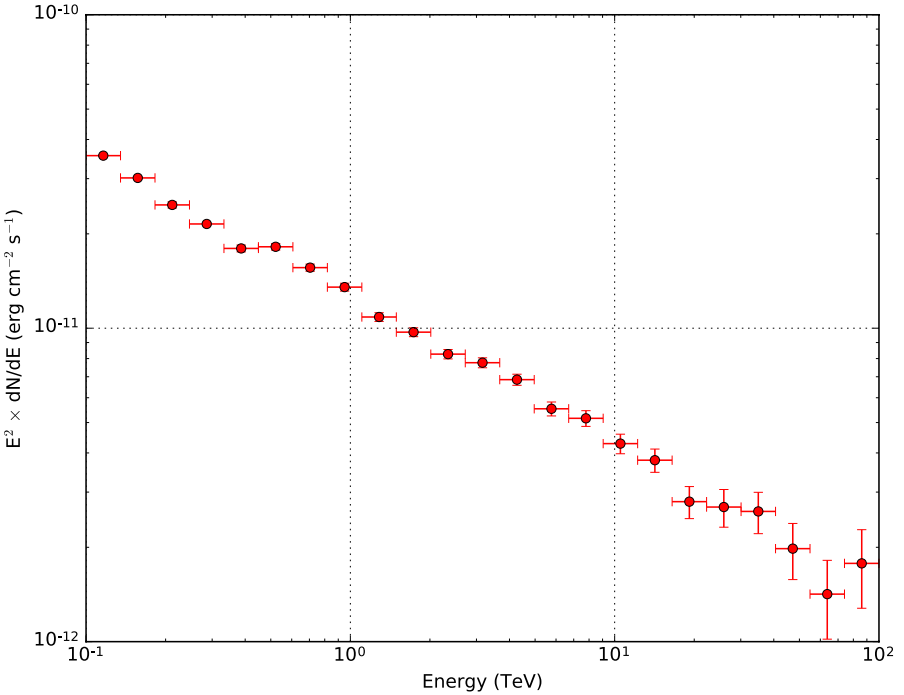

Comparison between simulated and reconstructed parameters

SNR name	$k_{0,\,\mathrm{in}}$ [$10^{-14}\,\mathrm{ph\,cm^{-2}s^{-1}\,TeV^{-1}}$]	$k_{0,\,\mathrm{out}}$ [$10^{-14}\,\mathrm{ph\,cm^{-2}s^{-1}\,TeV^{-1}}$]	γ_{in}	γ_{out}	σ_{in} [deg]	σ_{out} [deg]	$E_{\mathrm{cut,in}}$ [TeV]	$E_{\mathrm{cut,\,out}}$ [TeV]
RX J1713.7−3946	2300	2260 ± 10	2.06	2.06 ± 0.01			12.9	12.87 ± 0.34
HESS J1614+516	5780	5684.00 ± 52.00	2.46	2.46 ± 0.01	0.23	0.227 ± 0.001		
HESS J1731−347	467	455.00 ± 6.00	2.32	2.32 ± 0.01	0.22	0.219 ± 0.004		
					0.05	0.051 ± 0.008		
HESS J1800−240A	76.5	76.6 ± 2.00	2.5	2.56 ± 0.02				
W 49B	31.5	32.79 ± 1.32	3.14	3.07 ± 0.04				
HESS J1912+101	350	333.47 ± 6.05	2.7	2.67 ± 0.01	0.26	0.244 ± 0.003		
HESS J1745−303	284	279.32 ± 6.28	2.71	2.72 ± 0.01	0.20	0.204 ± 0.003		
W 28	75	122.59 ± 3.26	2.66	2.71 ± 0.02	0.17	0.108 ± 0.002		
W 51C	97	96.60 ± 3.20	2.58	2.56 ± 0.03	0.12	0.119 ± 0.003		

Table 1.3: All simulated and reconstructed parameters of the sources. From left to right: source name, simulated Prefactor, reconstructed Prefactor, simulated power law index, reconstructed power law index, simulated spatial extension, and reconstructed spatial extension. Pivot energy $E_0 = 1\,\mathrm{TeV}$.

SNR's SED and CTA Sensitivity

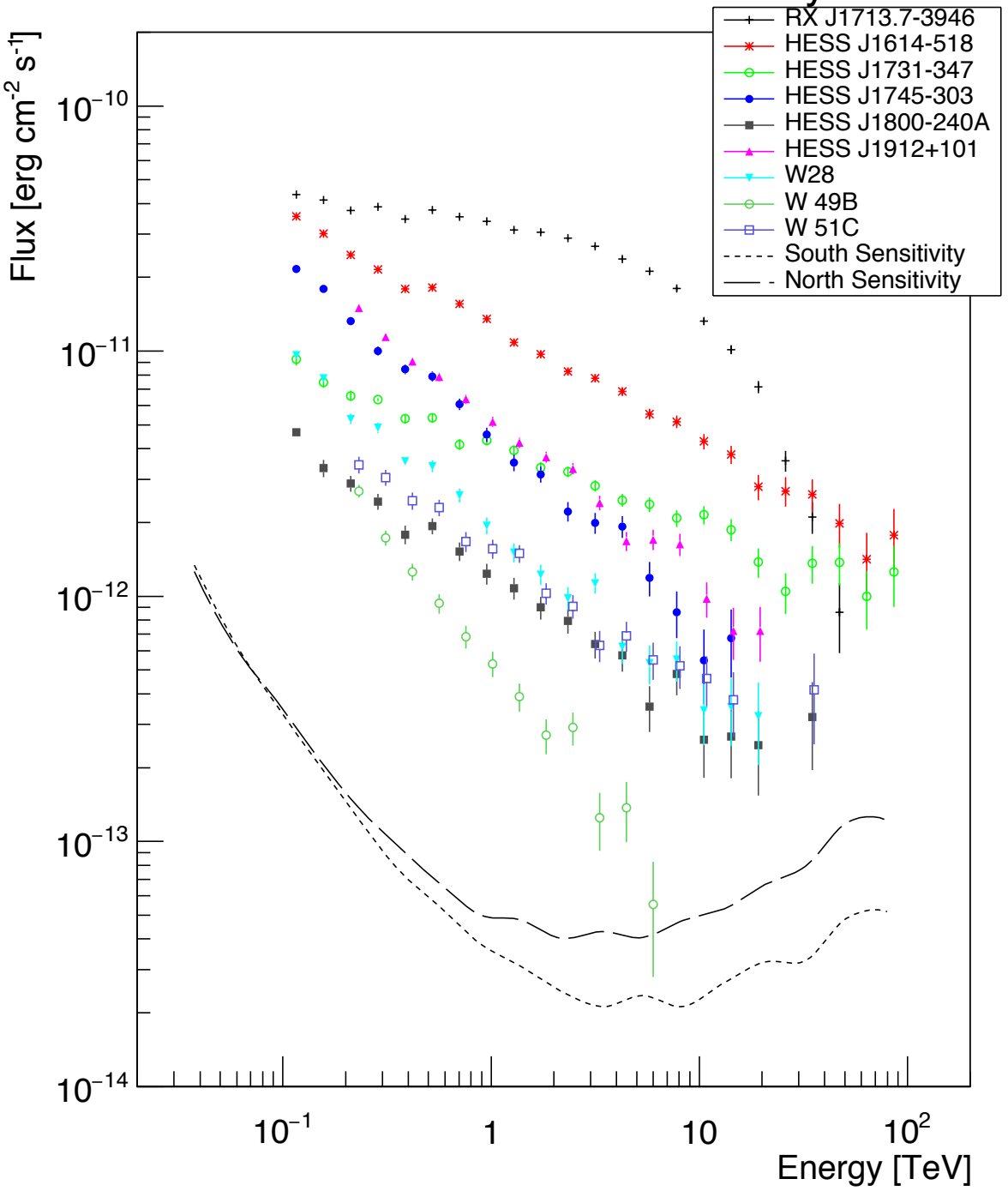

Visibility from TeVCat

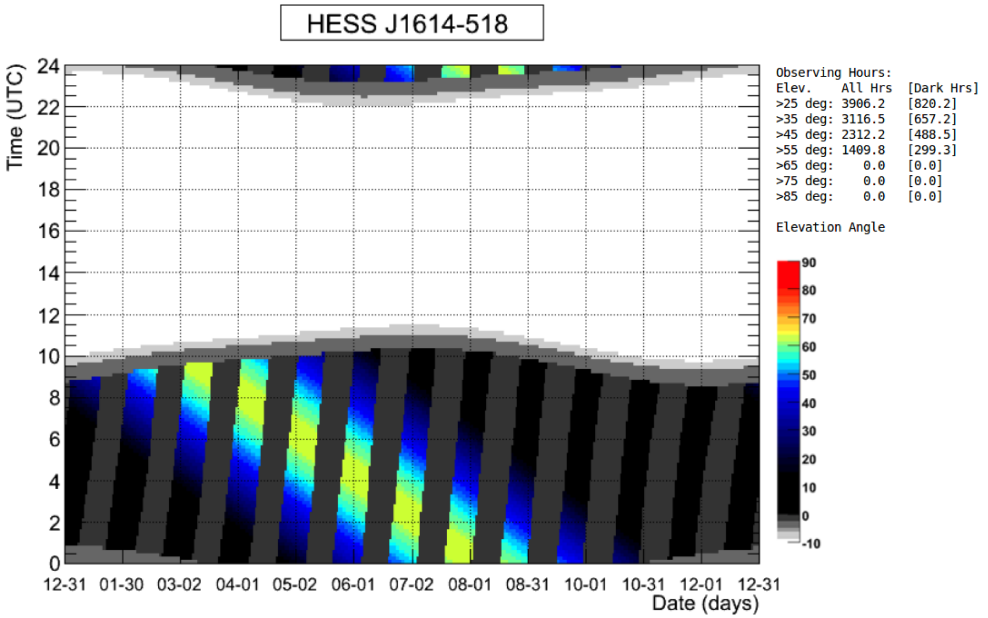

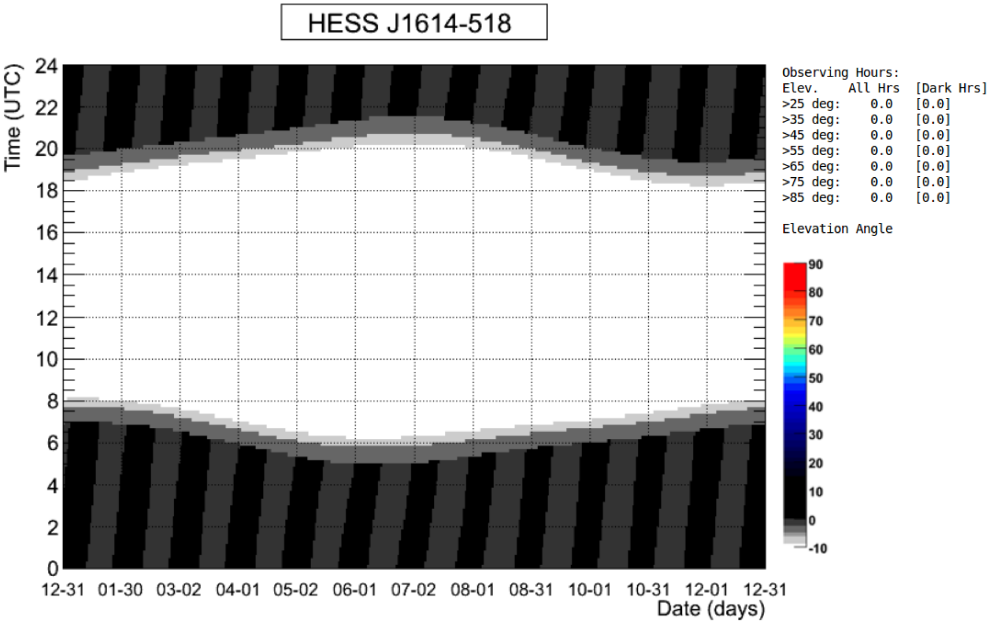

55 degree as threshold Elevation Angle value

As a conclusion, HESS J1912+101, W 49B and W51C are visible in the CTA northern site.

All candidates are visible in the CTA southern site.

In the analysis, we divide the sources into three groups:

- (1) sources with X-ray, *Fermi*-LAT and DC-1 data, including RX J1713.7−3946, HESS J1731−347 and W 49B, for which both the synchrotron and high-energy components of the model are constrained;
- (2) sources with *Fermi*-LAT data and DC-1 data, including HESS J1745−303, HESS J1800−240A, W 28 and W 51C, for which only the high-energy component is constrained;
- (3) sources with DC-1 data, including HESS J1614−518 and HESS J1912+101,

For group (1), we fit the data with hybrid lepto-hadronic model (IC and PI), with eight free parameters. For group (2), we follow the same approach as what we do for group (1), except that we freeze the parameters related to leptonic process and fit the other parameters. For group (3), we fit with a purely leptonic model and a purely hadronic model separately.

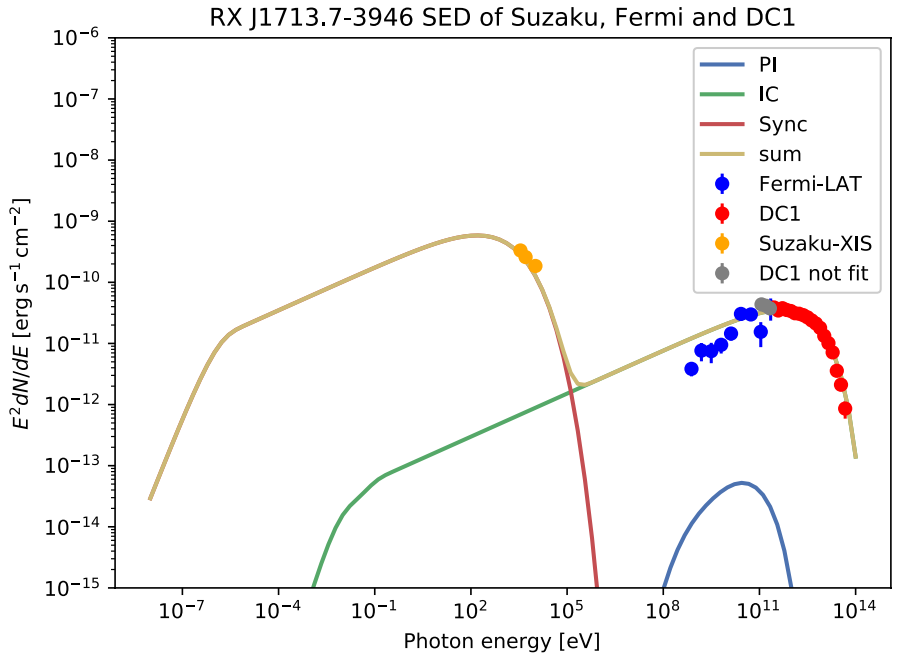

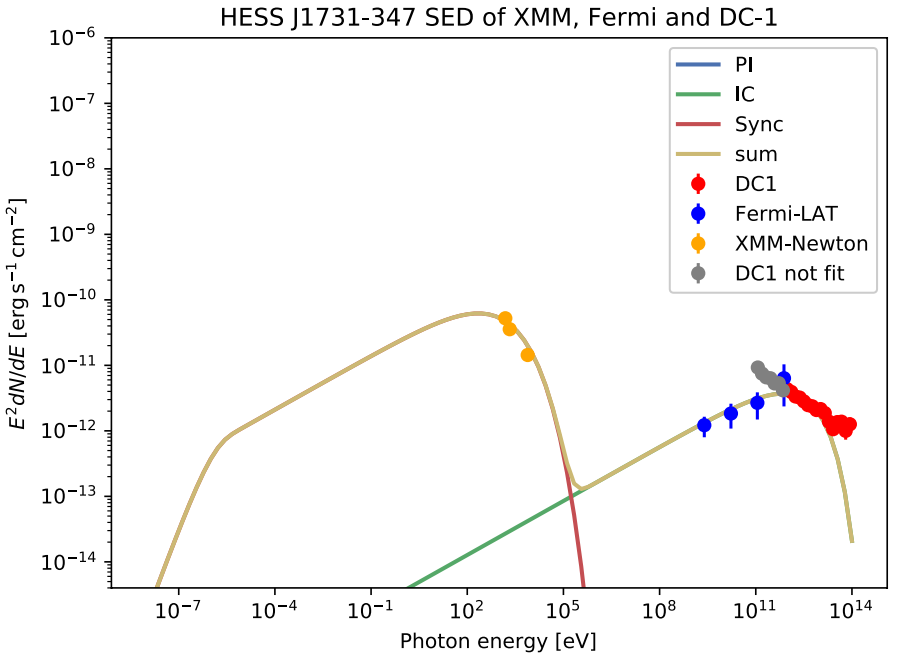

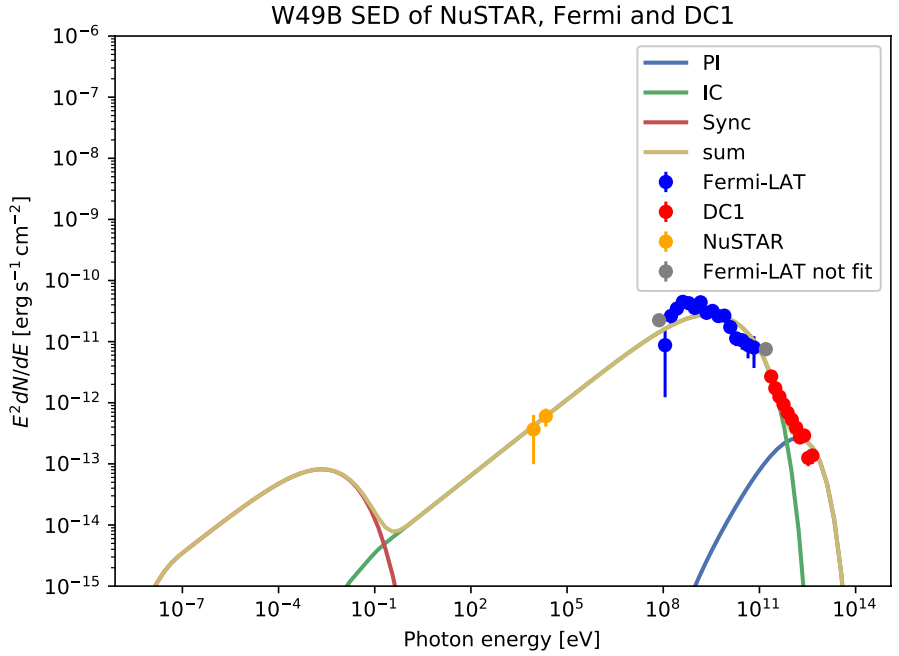

Group (1): DC-1, Fermi-LAT, and X-ray data

- Not promising PeVatron candidates
- W 49B has significant hadronic component

Since group (2) sources have DC-1 data and *Fermi*-LAT data only, we use two different methods to analyze them. On one hand, we perform the same analysis as for group (1), on the other hand, we freeze the parameters related to leptonic model to get the fitting results of hadronic model. In the latter case, five parameters related to IC are frozen:

- $\alpha_e = 2.5$
- $E_{\rm cut,e} = 10\,{\rm TeV}$
- $B = 70\,\mu{\rm G}$
- $K_{\rm ep} = 0.1$ Consider cosmic-rays abundance
- $N_{\rm H} = 100\,{\rm cm}^{-3}$ Typical value for SNR-MC systems

Reasonable values also from similar fitting work in other references

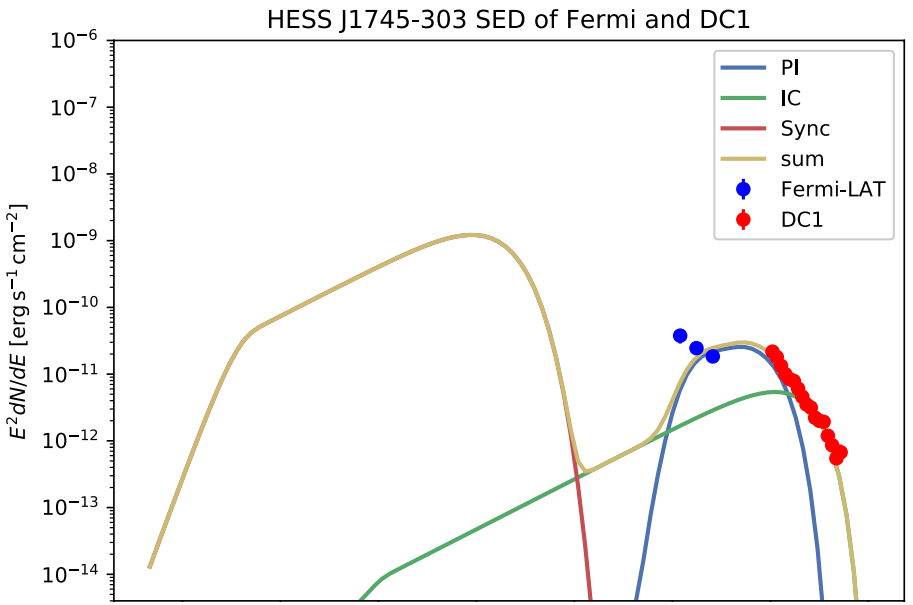

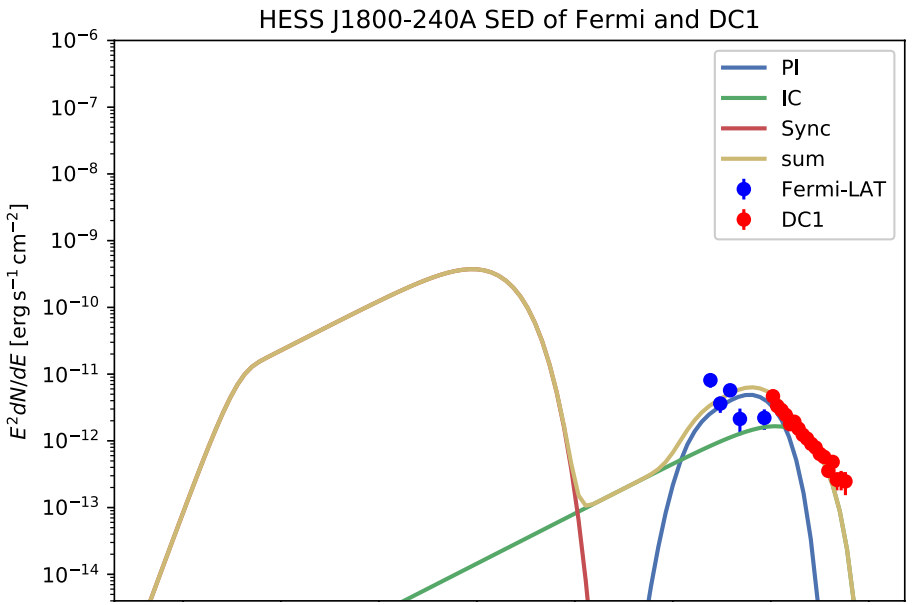

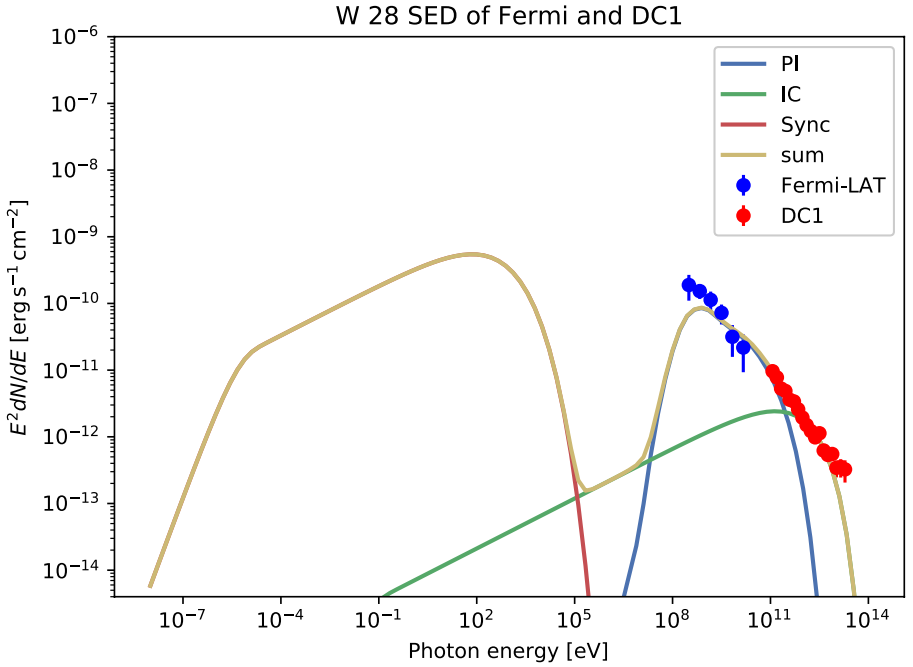

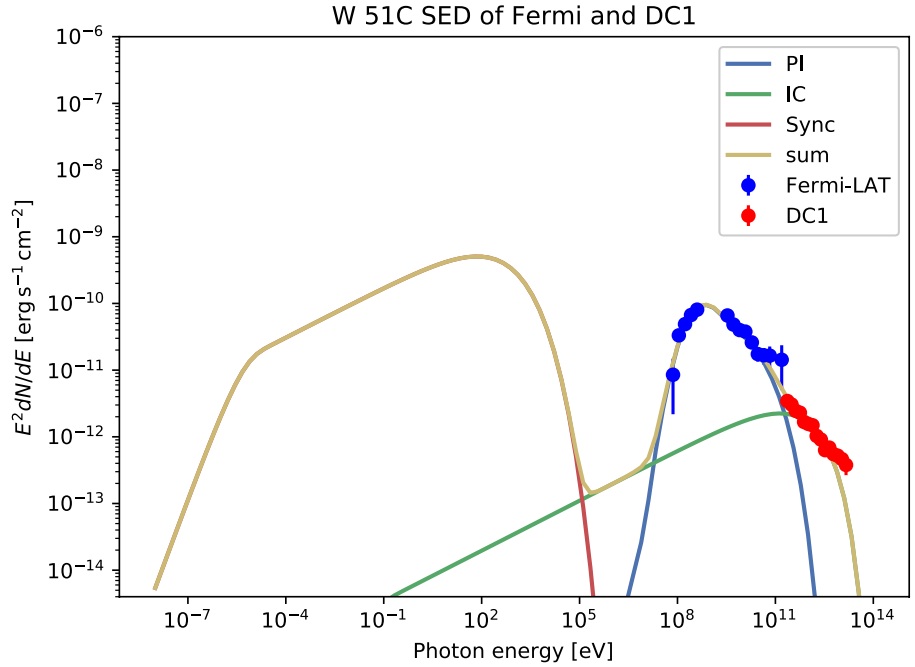

Group (2): DC-1 and Fermi-LAT data

- Not promising PeVatron candidates
- A hadronic contribution corresponding to ~ 1TeV proton

Best-fit parameters from Naima

SNR name	K_{ep}	$\log_{10} A_p$ [TeV^{-1}]	α_e	α_p	$\log_{10} E_{cut,e}$ [TeV]	$\log_{10} E_{cut,p}$ [TeV]	B [μG]	N_H [cm^{-3}]
RX J1713.7−3946	0.06 ± 0.01	47.99 ± 0.05	2.53 ± 0.02	1.27 ± 0.16	1.503 ± 0.016	-0.21 ± 0.05	17.29 ± 0.15	0.08 ± 0.02
HESS J1731−347	0.42 ± 0.12	47.09 ± 0.10	2.45 ± 0.11	1.0 ± 0.6	1.51 ± 0.06	0.12 ± 0.08	16.8 ± 0.5	0.04 ± 0.03
W 49B	0.61 ± 0.15	49.85 ± 0.14	2.17 ± 0.03	0.10 ± 0.04	-0.28 ± 0.02	1.02 ± 0.09	0.27 ± 0.11	0.004 ± 0.001
HESS J1745−303	0.09 ± 0.02	48.72 ± 0.10	2.92 ± 0.06	2.2 ± 0.7	0.64 ± 0.05	0.69 ± 0.19	56 ± 18	0.004 ± 0.001
HESS J1745−303 *		47.86 ± 0.02		1.91 ± 0.03		0.09 ± 0.03		
HESS J1800−240A	0.82 ± 0.18	47.28 ± 0.12	1.9 ± 0.2	0.15 ± 0.16	0.07 ± 0.07	1.18 ± 0.09	3 ± 2	0.07 ± 0.03
HESS J1800−240A *		47.35 ± 0.02		1.64 ± 0.06		-0.09 ± 0.03		
W 28	0.30 ± 0.09	47.78 ± 0.11	3.98 ± 0.05	2.7 ± 1.3	2.3 ± 0.3	2.1 ± 0.8	29 ± 12	0.04 ± 0.02
W 28 *		47.45 ± 0.02		2.03 ± 0.07		-0.03 ± 0.03		
W 51C	0.49 ± 0.09	49.00 ± 0.19	2.94 ± 0.15	1.10 ± 0.12	-0.02 ± 0.14	1.82 ± 0.17	15 ± 8	0.04 ± 0.01
W 51C *		48.15 ± 0.02		2.48 ± 0.01		-0.16 ± 0.05		

Table 1.3: Best-fit parameters for group (1) and (2). From the left to the right are the SNRs' name, ratio between electron and proton, proton amplitude, electron distribution index, proton distribution index, electron spectrum cutoff energy, proton spectrum cutoff energy, magnetic field, and target proton density. * indicates that we freeze the parameters related to electrons.

Summary

- The reconstructed parameters are modelled in good agreement.
- MWL data are essential to distinguish a lepto-hadronic model from a pure hadronic model.

Future

- Multi-wavelength program of CTA
  - magnetic field amplification
  - morphological correlation between gamma-ray and X-ray
- Possible Improvement for DC-1
  - consider the physical parameters for DC-2 simulation
  - parameters from current IACT observations